Electronic structure of copper phthalocyanine

Evangelista, Fabrizio; Carravetta, Vincenzo; Stefani, Giovanni; Jansik, Branislav; Alagia, Michele; Stranges, Stefano; Ruocco, Alessandro

Published in:
Journal of Chemical Physics

DOI:
10.1063/1.2712435

Publication date:
2007

Electronic structure of copper phthalocyanine: An experimental and theoretical study of occupied and unoccupied levels

Fabrizio Evangelista, Vincenzo Carravetta, Giovanni Stefani, Branislav Jansik, Michele Alagia, Stefano Stranges, and Alessandro Ruocco

Citation: The Journal of Chemical Physics **126**, 124709 (2007); doi: 10.1063/1.2712435
View online: https://doi.org/10.1063/1.2712435
View Table of Contents: http://aip.scitation.org/toc/jcp/126/12
Published by the American Institute of Physics

Electronic structure of copper phthalocyanine: An experimental and theoretical study of occupied and unoccupied levels

Fabrizio Evangelista[a)]
Dipartimento di Fisica, Università Roma Tre, via della Vasca Navale 84, I-00146 Roma, Italy

Vincenzo Carravetta
IPCF-CNR, via Moruzzi 1, 56124 Pisa, Italy

Giovanni Stefani
Dipartimento di Fisica, Università Roma Tre, via della Vasca Navale 84, I-00146 Roma, Italy and Unità CNISM, Università Roma Tre, via della Vasca Navale 84, I-00146 Roma, Italy

Branislav Jansik
IPCF-CNR, via Moruzzi 1, 56124 Pisa, Italy

Michele Alagia
ISMN-CNR, Sezione Roma1, Piazzale Aldo Moro 5, I-00185 Roma, Italy and Laboratorio Nazionale TASC-CNR SS-14, Km 163.5, Basovizza, I-34012 Trieste, Italy

Stefano Stranges
Dipartimento di Chimica, Universitá di Roma "La Sapienza" and INSTM Unita' di Roma1, Piazzale Aldo Moro 5, I-00185 Roma, Italy

Alessandro Ruocco
Dipartimento di Fisica, Università Roma Tre, via della Vasca Navale 84, I-00146 Roma, Italy and Unità CNISM, Università Roma Tre, via della Vasca Navale 84, I-00146 Roma, Italy

(Received 19 October 2006; accepted 5 February 2007; published online 29 March 2007)

An experimental and theoretical study of the electronic structure of copper phthalocyanine (CuPc) molecule is presented. We performed x-ray photoemission spectroscopy (XPS) and photoabsorption [x-ray absorption near-edge structure (XANES)] gas phase experiments and we compared the results with self-consistent field, density functional theory (DFT), and static-exchange theoretical calculations. In addition, ultraviolet photoelectron spectra (UPS) allowed disentangling several outer molecular orbitals. A detailed study of the two highest occupied orbitals (having a_{1u} and b_{1g} symmetries) is presented: the high energy resolution available for UPS measurements allowed resolving an extra feature assigned to vibrational stretching in the pyrrole rings. This observation, together with the computed DFT electron density distributions of the outer valence orbitals, suggests that the a_{1u} orbital (the highest occupied molecular orbital) is mainly localized on the carbon atoms of pyrrole rings and it is doubly occupied, while the b_{1g} orbital, singly occupied, is mainly localized on the Cu atom. *Ab initio* calculations of XPS and XANES spectra at carbon *K* edge of CuPc are also presented. The comparison between experiment and theory revealed that, in spite of being formally not equivalent, carbon atoms of the benzene rings experience a similar electronic environment. Carbon *K*-edge absorption spectra were interpreted in terms of different contributions coming from chemically shifted C 1*s* orbitals of the nonequivalent carbon atoms on the inner ring of the molecule formed by the sequence of CN bonds and on the benzene rings, respectively, and also in terms of different electronic distributions of the excited lowest unoccupied molecular orbital (LUMO) and LUMO+1. In particular, the degenerate LUMO appears to be mostly localized on the inner pyrrole ring. © *2007 American Institute of Physics*. [DOI: 10.1063/1.2712435]

I. INTRODUCTION

Metal-phthalocyanines (MPc) are among the most studied organic molecules in the ever moving front of organic semiconductors. This class of materials, also including polyacenes, thiols, and fullerides, can show interesting electronic properties: high hole mobility in well-ordered thin films,[1] self-assembling behaviour from the very first growth stages,[2] conduction and superconduction upon suitable alkali doping.[3]

MPcs are planar fourfold-symmetry molecules characterized by a common electronic structure of the ligand independent from the metal in the center.[4] In particular, the energy gap in the ligand between the highest (doubly) occupied molecular orbital (HOMO) (with a_{1u} symmetry) and the lowest unoccupied molecular orbital (LUMO) (e_{2g}) falls in the visible region. The peculiarity of copper-phthalocyanine (CuPc)

[a)]Present address: Zernike Institute for Advanced Materials, Rijksuniversiteit Groningen Nijenborgh 4, 9747 AG Groningen, the Netherlands.

is that the Cu-derived outer level (with b_{1g} symmetry) is predicted to lie, singly occupied, in the HOMO-LUMO ligand gap and the corresponding orbital can be addressed as singly occupied molecular orbital (SOMO).[5] The single occupancy of the Cu-derived level was proved by the XANES observation of the Cu $L_{2,3}$ edge[6,7] associated to a Cu $2p$-b_{1g} transition, otherwise impossible to occur. MPcs also show attracting structural properties: they can grow in an ordered way, forming stacked weakly interacting columns, eventually exhibiting different orientations (and different molecular orbitals' overlap) with respect to the surface.

It appears evident how mastering the processes that induce molecular ordering on a surface represents a great challenge in view of technological spin-offs and also to reach a complete understanding of organic-inorganic interface processes. Such skills can be gained once the role of the molecule-substrate interaction is understood. Several mechanisms occurring at the interface can characterize an MPc-substrate interaction, such as charge transfer,[8] interface dipoles,[9,10] and new interface-localized electronic states.[11] In order to shed light on the nature of the interaction at the interface, a detailed description of the electronic structure of the CuPc molecule needed. Indeed, by comparing the interface with the isolated molecule, contributions coming from the molecule rather than from the interaction with the substrate will be singled out.

Several theoretical works addressed the electronic structure of phthalocyanines by means of different methods, the most recent ones taking into account electronic correlation, providing a satisfying energy level scheme of the neutral molecule.[4,12] Density functional theory (DFT) method was successfully employed also in predicting the valence band of a lead-Pc film[13] with particular attention devoted to the different contribution coming from the electronically inequivalent C and N atoms in the molecule. A recent work coupling experiment and theory reports on a weak intermolecular interaction in CuPc crystals,[14] while DFT calculations proved to be successful in describing a x-ray absorption near-edge structure (XANES) spectrum from the N *K*-edge spectrum from free[15] and iron[16] phthalocyanine derivatives.

We also believe that a satisfying knowledge of the electronic structure of a large organometallic molecule can be better reached by means of a joint experimental and theoretical investigation. In the field of x-ray spectroscopies, only recently it was possible to pursue theoretical approaches allowing the description of not only the ground state of the molecular system but also its high excited states. In particular, the static-exchange (STEX) approximation approach that we are referring to[17] allows simulating an experimental x-ray absorption (XANES or near-edge x-ray absorption fine structure) spectrum. Such a theoretical approach revealed to be successful in disentangling different C contributions to XANES spectra of large organic molecules such as, for instance, heterocyclic molecules,[18,19] and planar π-conjugated systems such as pentacene,[20] encouraging us to apply the same method to a much more complex system such as a metal phthalocyanine.

From an experimental point of view, in spite of the acknowledged importance of knowing the phthalocyanine electronic structure, experimental literature on isolated MPcs is quite poor. Electron diffraction studies on metal phthalocyanines aimed at the description of the molecular structure,[21,22] while a few photoemission experiments addressed the electronic structure. In the work by Berkowitz[23] an overview of different UPS spectra of transition-metal Pcs was reported, while Schlettwein *et al.*[24] focused their attention on the comparison between isolated molecules and thin films, supported by theoretical calculations. A gas phase study was engaged also on Vanadyl Pc,[25] where a non-Aufbau filling was experimentally deduced and confirmed by theoretical calculations. To the best of our knowledge neither experimental nor theoretical results concerning CuPc core level spectra (e.g., C $1s$) as well as XANES of the isolated molecule are presently available.

In this work we report on an experimental and theoretical study on the CuPc molecule. By photoemission we addressed both the C $1s$ core level [by x-ray photoemission spectroscopy (XPS)] and the valence levels [by ultraviolet photoemission spectroscopy (UPS)]. The chemical selectivity of XPS allowed the investigation of the electronic environment of each atom, while UPS shed light on the nature of the outer molecular orbitals. A combined experimental and theoretical XANES study at the C *K* edge was engaged on the free molecule. In order to disentangle the different contributions to the spectra, experimental XPS and XANES spectra were simulated by means of a series of calculations based on *ab initio* methods: self-consistent field (SCF) for the photoemission and STEX[17] for the absorption spectra, particularly focused on singling out the different contributions from each chemically different carbon atom.

In the following two sections we will deal with the details about experimental measurements and computational procedures. Then spectroscopic results will be divided in UPS, XPS, and XANES parts, where the experiment-versus-theory approach provides insight on the electronic structure and on the molecular orbitals' spatial distribution.

II. EXPERIMENT

All measurements concerning the isolated molecule were performed at the Gas Phase beam line of the Elettra Synchrotron Light Laboratory (Trieste). The beam line is equipped with an undulator which delivers light in the range from 14 to above 1000 eV, with the help of a monochromator consisting of a plane mirror and five spherical gratings. The beam line is presently equipped with several different interchangeable apparatuses. The results presented in this work have been obtained using the ARPES end station.[26] Photoelectron spectra were recorded using a hemispherical electron energy analyzer (VSW, 50 mm of mean radius and 1.5 mm of exit slit) operated in constant pass energy mode. When working in high resolution conditions (i.e., UPS measurements), a pass energy of 5 eV was employed yielding an overall (photon+analyzer) energy resolution of less than 100 meV. For core level photoemission spectra a pass energy of 10 eV was employed, which implied (when coupled to the resolving power of the beam line at the photon energy of about 300 eV) an overall resolution of about 300 meV. The

kinetic energy scale of the analyzer was calibrated by introducing suitable gases (e.g., CO_2) into the ionization region together with the sample and recording a photoelectron spectrum at the same photon energy. In particular, the C 1*s* XPS was collected with a photon energy of 309.5 eV with the ionization energy scale calibrated against the binding energy of the C 1*s* of CO_2 gas [BE=297.65 eV[27] (BE denotes binding energy)]. High-resolution x-ray absorption spectra were collected in total ion-yield mode. A channeltron acts as a detector for positively charged ions coming from the interaction region. The energy resolution for XANES measurements is only limited by the photon energy bandpass used, namely, about 40 meV at 300 eV. Also in this case the energy scale was calibrated according to C *K* edge spectrum measured for CO_2.[28] For the C 1*s* XPS spectrum and for the highest band of the high resolution UPS spectrum a fitting procedure was performed. Every spectral component is described with a Voigt profile, as a result of the convolution of a Gaussian function and of a Lorentzian profile, which are related to the experimental resolution and the natural lifetime of the excitation, respectively. The width of the Gaussian was kept equal for all the components, while the Lorentzian width was kept fixed to the value of 150 meV for C 1*s*, a value that was also used for fits in CuPc films.[7]

Commercial sublimated CuPc was obtained from Aldrich Chemical (99.7% dye content, already purified) and introduced in the oven present in the experimental chamber. Vaporization in the ionization region was achieved by heating the oven at a suitable temperature: a value of about 350–400 °C was reached, with no traces of molecular decomposition found at this temperature.

In this paper, photoelectron spectra (from both core levels and valence band) on copper Pc thick films deposited on Au(110) performed at the ALOISA beam line are also presented. Details about this experiment and the experimental setup are given elsewhere.[7] For the aim of this work it will be sufficient to remark that the nominal coverages here reported are always above 40 Å, a thickness for which we can safely consider the molecules to be scarcely affected by the substrate. The XPS spectrum was realized with a photon energy of 500 eV with the binding energy scale calibrated against the Au 4*f* core level peaks.

III. COMPUTATION

A. Geometry

Geometry optimization of CuPc was performed by ground state SCF calculations employing GAMESS[29] and the TZV basis set (C[5*s*,3*p*],H[3*s*]). The only restriction on the system geometry was to be planar. Molecular planarity was adopted as a simplifying model for the real system, where copper atom should be actually positioned slightly above the carbon-nitrogen ring plane. In this way, the symmetry of the system was artificially increased, thus reducing computational costs, without any consequence on the quality of the theoretical results presently considered as they involve deep core levels of carbon atoms. As a result, only four nonequivalent C atoms, numbered from 1 to 4 in the insert of Fig. 2 could be considered.

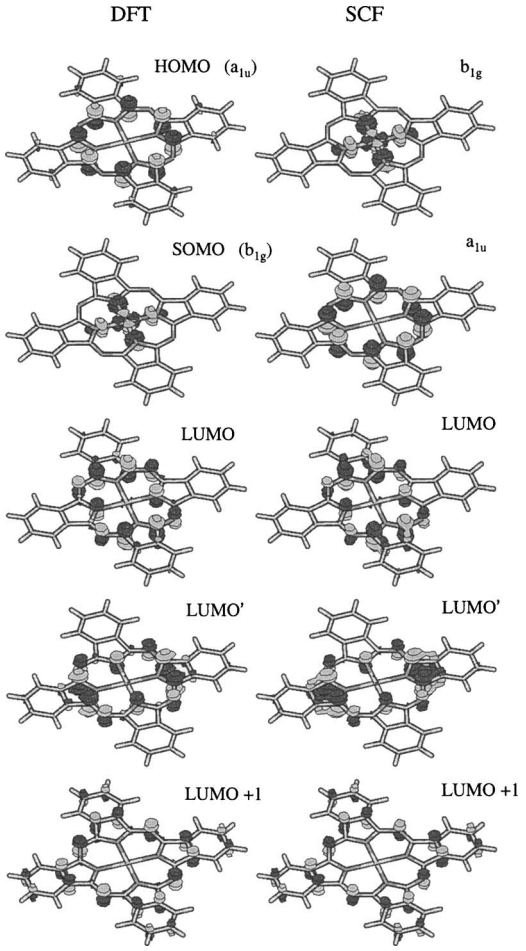

FIG. 1. Spatial distributions of the highest occupied (HOMO, a_{1u} symmetry, and SOMO, b_{1g} symmetry) and lowest unoccupied (LUMO) CuPc molecular orbitals. DFT calculations are on the left half of the figure, while SCF results are on the right half. Although a_{1u} and b_{1g} orbitals appear to be energy swapped in the two calculations, the electron distribution of the unoccupied orbitals is identical.

B. SCF and DFT calculated molecular orbitals

It is worth discussing at this stage the shape of the outer molecular orbitals as they appear by DFT and SCF calculations. The ground state and some excited states of phthalocyanines were investigated by several theoretical approaches,[30] the most recent calculations[4,12] being done at a DFT level. It is commonly accepted that the SOMO of CuPc (which is an open shell system) is essentially located on the Cu atom with a main $3d(x^2-y^2)$ component mixed with small contributions from the in-plane N 2*p* orbitals of the ligand atoms. The HOMO is instead mainly localized on the carbon atoms of pyrrole rings (see Fig. 1) with contributions from the 2*p* orbitals orthogonal to the molecular plane. Our DFT calculations with the B3LYP functional and a large basis set (Ahlrich PVTZ C[5*s*,3*p*,1*d*], H[3*s*,1*p*]) confirm this picture with the SOMO being 1.5 eV higher than the HOMO, in agreement with previous calculations on CuPc.[4] The DFT-calculated distributions can be seen in the left side of Fig. 1 where the spatial distributions of the highest occupied and the lowest unoccupied (degenerate LUMO and LUMO+1) orbitals are also presented. The SCF calculations show an inversion of the Cu-derived (b_{1g}) and the ligand-

derived (a_{1u}) levels (the former is now 5.5 eV lower) that is not unusual when a method neglecting the electron correlation is adopted for a molecule with a high density of orbital levels close to the ionization threshold. In Fig. 1 we can also observe that the virtual orbitals relevant in the photoabsorption spectrum (LUMO, LUMO′, and LUMO+1) are, anyway, not affected by this $a_{1u}-b_{1g}$ level inversion, actually revealing the same electronic structure when computed both at the DFT and at the SCF level (right side of Fig. 1). This means that we can safely employ the SCF calculations as our basis for the STEX procedure to be presented later on.

Every molecular orbital is not homogeneously distributed over all atoms in the molecule. In particular, whereas the b_{1g} (SOMO) level is strongly concentrated in the central Cu atom (with significant N contribution), the a_{1u} (HOMO) orbital is mainly localized on C atoms in pyrrole rings (C4 atoms). The electron density distribution of the a_{1u} orbital is of crucial importance when interpreting the high resolution UPS spectrum, as well as the localization of the LUMO orbitals (also concentrated in the inner pyrrole ring) will provide a tool to interpret the spectral density of the C *K*-edge XANES spectra.

C. XPS spectra

The CuPc ground state wave function was optimized by the restricted open shell Hartree-Fock procedure using a locally modified version of DALTON program.[31] The 1*s* core orbitals on all symmetry distinct carbon atoms were localized using Boys localization procedure. The core-ionized states were then optimized by a two-step procedure restarting from the ground state wave function. In the first step the singly occupied core orbital (or core hole) was left out of the optimization, while all orbitals were optimized in the potential of the core hole. In the second step, the core orbital was optimized, while all the remaining orbitals were left out of optimization. Due to the presence of two (core and valence) open shells, two spin couplings (singlet and triplet) can be realized, and both singlet and triplet states were initially computed. It turned out, however, that the singlet-triplet splitting of these states was negligible (<1 meV), hence only singlet states were considered. The corresponding orbital set was employed to build both the singlet and triplet ionized wave functions. Symmetry distinct atoms of the same species in a molecule give origin to chemically shifted contributions to the XPS spectrum. As already discussed, we considered that core ionization leads only to four distinct core-ionized states. These can be divided in atoms belonging to benzene rings (C1, C2, and C3) and atoms located in the pyrrole rings (C4) (see Fig. 2).

Calculations of the reference ground and core-ionized states were carried out employing the PVTZ basis set $(C[5s,3p,1d],H[3s,1p])$ i.e., triple zeta plus polarizing and diffuse functions. The Ahlrich triple zeta basis set spans 686 basis functions on our system, which gives rise to a very large number of two-electron integrals. As our code was not able to carry out direct integral evaluation for the calculation of core-ionized states of an open shell molecule, the integrals were stored on disk, employing Huffman compression algorithm of the zlib library.

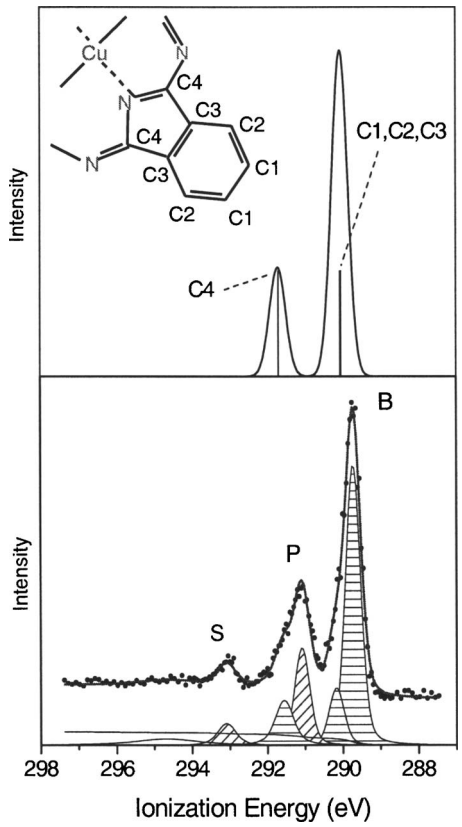

FIG. 2. C 1*s* core level XP spectrum. Lower panel: gas phase experimental with superimposed results of the fitting procedure (see Table I). Upper panel: theoretically simulated spectrum with vertical bars indicating the single carbon atom contributions.

D. XANES spectra

XANES spectra were obtained within the static exchange STEX[17] approximation. The STEX approach consists in a separate states calculation in which the ground state is approximated by the SCF wave function, while the excited state is approximated by the coupling of a relaxed target ionic state and an excited orbital optimized in the static field of the molecular ion. This is the eigenvector of a one-particle Hamiltonian that describe the motion of the excited electron in the field of the remaining molecular ion corresponding to a specific core hole. In this way the full, discrete, and continuum x-ray photoabsorption spectrum for each core-excitation site was obtained from singly excited configurations using the virtual orbitals of the specific core-ionized system. While the electronic relaxation around the core hole is fully taken into account by the SCF procedure and it is assumed to be independent on the excited electron (with the excitation levels converging to a common ionization limit); electron correlation effects and the screening effect of the excited electron are neglected. This may be considered the most relevant approximation of this *ab initio* approach, because the interchannel coupling between different core-excitation channels, also neglected, is indeed very small for core excitations due to a significant energy and/or spatial

separation between core holes in most of the molecular systems. For the lowest core excited states of valence, often π character, an overscreening effect takes place. Then, when comparing experiment and theory it is important to consider that, as a consequence of the STEX approximation, the energy scale of the calculated spectra will be compressed against the ionization potential edge. In fact, by neglecting the interaction between the excited electron and the remaining electrons on the target, the potential due to ionic charge distribution is less attractive than it should be. Due to this, the lower excited states are less bound and, hence, closer to the ionization potential energies. In order to correctly compare the experimental spectrum and the theoretical calculation a "decompression" factor was employed. It is generally assumed that the overscreening error is constant for the different ionization channels, even if this is not always strictly true (e.g., when relaxation effects are particularly different for different chemically shifted atoms). The excitation energies of the XANES spectrum were obtained by adding the ionization potential to the STEX eigenvalues and the corresponding transition moments were obtained as dipole matrix elements (in length gauge) between ground state and STEX final states projected on nonorthogonal sets of molecular orbitals.

IV. XPS: EXPERIMENTAL AND THEORETICAL RESULTS

A. C 1*s*

The photoelectron spectrum from the C 1*s* core level is reported in the lower panel of Fig. 2. The spectrum shows two main peaks at about 289.75 eV (B) and 291.1 eV (P) ionization energy (IE) and a weaker feature at 293.1 eV (S). Carbon atoms in phthalocyanines can be, in first approximation, divided in two inequivalent groups as displayed in the insert of the upper panel: C atoms in the pyrrole ring (C4 atoms, P) will exhibit an electronic charge density that is positive with respect to benzene ring (C1, C2, and C3 atoms, B).[32] As a consequence, photoemission from C1, C2, and C3 carbon atoms is expected to occur at a lower ionization energy compared to the C4 ones. The weaker structure located at IE of about 293.1 eV (S) stems from a two-electron process, known as a shake-up satellite, involving a HOMO-LUMO transition.

Further insight in the spectral density can be gained by means of a fitting procedure, whose results are reported in Table I. To properly describe the XPS spectrum, five components are needed: two located in the benzene region, two in the pyrrole region, and one to reproduce feature S. The components under the pyrrole peak are located at 291.11 eV (P) and 291.62 eV; the latter is separated from the main component of peak B of about 1.9 eV thus suggesting an assignment in terms of a shake-up satellite (S_B) associated to benzene rings. In the benzene region the main component (B) is centered at 289.74 eV, while a second component (B′) is found at 390 meV from the main line. This could be interpreted as a further electronic inequivalence in the benzene rings, even if the intensity ratio of B and B′ is not in favour of this hypothesis. Alternatively it could be ascribed to a C–H vibrational mode associated to electron emission from C 1*s* level, as also suggested by a recent work on lead phthalocyanine.[13] Such a vibrational mode is known to be located 380 meV from the main line, a value very close to that derived from our fitting procedure.

TABLE I. Numerical parameters corresponding to the fitting procedure presented in the upper panel of Fig. 2. The best fit was obtained by assigning two different Lorentzian widths to the two shake-up satellites. This can be explained with the neglect of possible vibrational modes falling in the P peak IE region.

	BE	A	LW	GW
B	289.74	1	0.15	0.35
B′	290.13	0.25	0.15	0.35
P	291.11	0.43	0.15	0.35
S_B	291.62	0.18	0.35	0.35
S_P	293.10	0.09	0.19	0.35

Further information on the origin of peak B′ can be deduced from the theoretically calculated C 1*s* XPS spectrum. A convolution of the XPS theoretical spectrum (bar diagram) with a Gaussian function of FWHM=0.5 eV (FWHM denotes full width at half maximum) is presented in the upper panel of Fig. 2 to simulate the effect of both the limited experimental resolution and the vibrational broadening. The theoretical XPS spectrum compares quite well to the experimental one, except for an energy shift stemming from neglecting the electron correlation and, due to the type of computational method adopted, the absence of the shake-up satellite. We observe that, in spite of the formal nonequivalence of the C1, C2, and C3 atoms, only two different core ionization potentials are indeed predicted by calculations. C atoms located in the pyrrole rings (C4) are significantly perturbed by two adjacent nitrogen atoms and are also affected by the presence of the central Cu atom. This is very well reflected by a calculated binding energy of 291.5 eV with a chemical shift that is particularly strong compared to values observed for other organic molecules. This can be ascribed to a strong bond polarization induced by neighboring nitrogen atoms, in agreement with Mullikan atomic charge calculations, which are of positive value for group 4 carbon atoms while they are negative for group 1–3 carbon atoms.

Additionally, the C 1*s* core levels from benzene rings have the same computed binding energy (290 eV), thus revealing a substantial equivalence among C1, C2, and C3 carbon atoms. Then, the picture of a nonequivalence in the C atoms of the benzene ring to explain the presence of the shoulder B′ seems to be unlikely, suggesting that the shoulder B′ has to be ascribed to an excitation of an in-plane C–H stretching vibrational mode after the excitation of the photoelectron from the C 1*s* level.

B. C 1*s*: Gas phase versus thin film

In Fig. 3 the superposition of the C 1*s* XPS spectrum of a thick CuPc film and the gas phase spectrum of Fig. 2 is presented. The two spectra are reported in binding and ion-

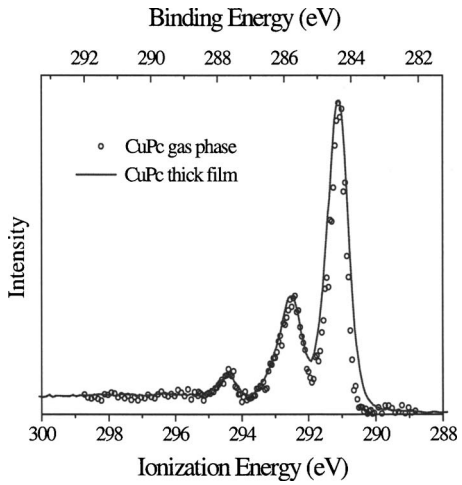

FIG. 3. Comparison between C 1*s* XP spectra collected in gas phase (lower energy scale) and on thick film (upper energy scale). Spectra were realigned to highlight lineshapes' differences.

ization energy scales, respectively, with the energy scales being offset one with respect to the other to better appreciate line shape differences.

The similarities between the two line shapes are striking: the three main structures (B, P, and S) are present at the same relative energy positions. This evidence implies two important facts about the electronic structure of the molecule. The preserved chemical shift between carbon atoms in benzene rings (B) and in pyrrole rings (P) suggests that the outer charge distribution around carbon atoms is not significantly changed in the condensed phase. As the shake-up satellite involves the HOMO-LUMO transition, a steady energy separation between peak S and its parent peak, lead us to conclude that no significant alteration of the electronic level diagram occurs moving from the isolated molecule to a thick film arrangement. The only difference visible in Fig. 3 is that in gas phase B and P are narrower spectrum than in the thick film, but this can be ascribed to the different overall energy resolution.

V. UPS EXPERIMENTAL RESULTS

The photoelectron spectrum taken at 21 eV of photon energy is reported in the upper part of the lower panel of Fig. 4. In order to gain information about the nature of these orbitals, a comparison with a UPS spectrum collected from CuPc thin films with photon energy of 210 eV is provided in the lower part of the panel with the binding energy scale aligned to the HOMO peak. Within the simplifying assumption that the molecule π levels follow the photoionization cross section of the C $2p$, these features are expected to quench with increasing the photon energy much more (two orders of magnitude) than the Cu d-derived states, thus modifying the relative intensities and the shape of the spectral density.[33,34]

As also shown in the previous XPS section, no significant changes in the electronic structure occur when we move from the isolated molecule to thick films. Thus, it is safe comparing spectra from both free molecules and films. Six

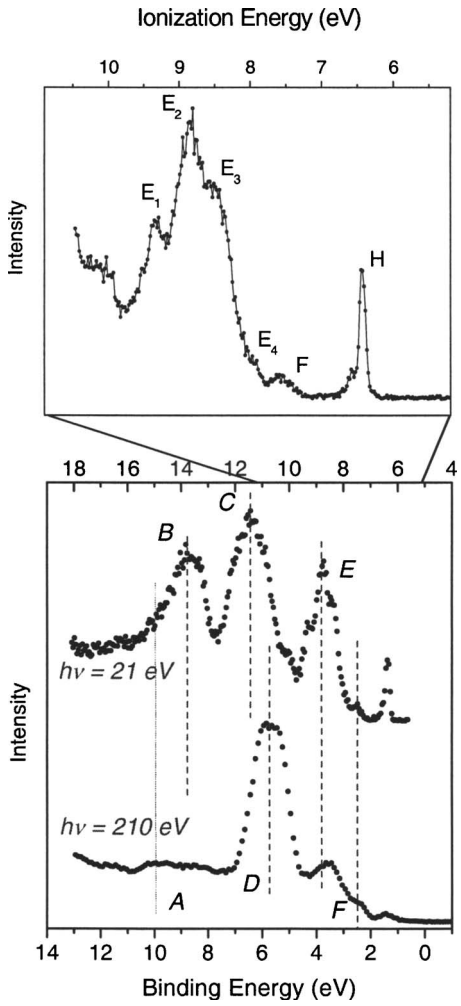

FIG. 4. Lower panel: CuPc gas phase UPS spectrum collected with a 21 eV photon energy (in ionization energy scale) compared with a CuPc thin film spectrum collected at $h\nu$=210 eV figure (in binding energy scale). Upper panel: high resolution photoelectron spectrum collected with a photon energy of 21 eV. Main structures are labelled with E_i, F, and H letters.

different states, whose evolution can be followed with the help of vertical dashed lines, are labelled from A to F in Fig. 4.

In the high ionization energy region the feature centered at 13.75 appears to be composed of two contributions, B and its shoulder A. While B is strongly reduced at 210 eV, the depression of A is less evident, thus allowing us to assign B as due to an orbital mostly delocalized on the molecular ring and to guess an important Cu contribution for A. At lower ionization energy a strong feature is centered at 11.45 eV (C) with a shoulder on its low IE side (D). At $h\nu$=210 eV this shoulder is the most important feature in the spectrum, while the C feature has disappeared. Here C can be ascribed to π levels, while D is a Cu-derived state, also in agreement with Berkowitz.[23]

In the low ionization energy region, the wide feature centered at about 8.8 eV (E), reduces its intensity with increasing $h\nu$. On the other hand, located at 7.6 eV IE, there is a weak feature for $h\nu$=21 eV (F) that does not vanish and, on the contrary, exceeds the a_{1u} (HOMO) intensity at an

ionization energy of about 6.4 eV for $h\nu$=210 eV. Such a behavior leads us to think that the F peak is also due to the ionization of another copper-derived orbital.

To gain insight in this region we report in the upper panel of Fig. 4 a spectrum collected at a higher energy resolution than the more extended one presented in the lower panel. The higher resolution allows some fine structure to be better resolved; in particular, the wide structure centered at about 8.8 eV (IE) reveals to be composed of four distinct contributions, while the state at approximately 7.6 eV (IE) is clearly distinguishable. Labels referring to the main features discussed [$E_i(i=1-4)$, F, and H] are also reported. The three main contributions are located at 9.28 eV (E_1), 8.79 eV (E_2), and 8.46 eV (E_3) IE, with a weak shoulder (E_4) positioned at about 8 eV. The F structure is observable at 7.59 eV, while the HOMO level is detectable at 6.38 eV (H). We stress here the asymmetry of H towards higher IE that will be object of a deeper analysis in the next section.

Peak F has already been addressed as a copper-derived state. From DFT calculations on the neutral molecule[4] the highest Cu-derived orbital (SOMO) is seen to be located in the HOMO-LUMO energy gap. Then, a peak at lower IE with respect to the a_{1u} peak could be expected in the UPS spectrum. On the other hand, the ionization of the a_{1u} orbital, giving origin to a hole delocalized on the Pc ring could be considered more easily realized than that of the b_{1g} orbital strongly localized on Cu.[4] As a consequence, the energy of the b_{1g} hole state could also be expected to be higher than that of the a_{1u} hole state. This prediction perfectly matches the experimental finding of the Cu-3*d*-derived peak located at 7.59 eV (F), 800 meV above the a_{1u} peak on the ionization energy scale, which is in a reverse order with respect to the DFT orbital energy order in the neutral molecule. Alternatively, the experimental finding could also be interpreted in terms of a non-Aufbau filling of CuPc electronic levels as inferred in the case of the *V*OPc isolated molecule.[25] Despite the fact that our experimental data are compatible with both hypotheses, the only calculations concerning the ionization of copper-Pc complex seem to indicate that an a_{1u}-b_{1g} inversion takes place upon photoionization.[4]

No predictions of levels composing the E structure are available for CuPc, but they are for zinc-Pc.[12] From a comparison among the valence levels of several transition-metal phthalocyanines,[4] no significant changes for the ligand molecular orbitals are observed by varying the central metal atom. As a consequence we can be confident that good information for CuPc can be gained also from calculations performed on ZnPc. In this case electronic states below the a_{1u} energy position, are seen to group themselves around three mean ionization energies that can be considered to correspond to the complex band in our spectra: the relative differences in energy of the three main groups are in agreement with our experimental data. By these arguments we propose, keeping the Nguyen notation for Pc ligand-derived orbitals used for ZnPc,[12] an assignment of the bands E_3-E_4 in Fig. 4 to the ionization of $3b_{2u}$, $6e_g$, and $4a_{2u}$ orbitals, while E_2 is assigned to $5e_g$, $2b_{1u}$, and $3a_{2u}$ ionizations and the E_1 structure to the $1a_{1u}$ ionization.

A high resolution UPS spectrum in the region of the first ionized molecular orbital is presented in Fig. 5. The spectrum is dominated by one main feature ascribed to photoemission from the a_{1u} orbital and located at the ionization energy of 6.38 eV with some extra features detectable on the high binding energy side. A fitting analysis was performed and the resulting parameters are reported in Table II. Besides the main peak, two more components are needed to properly describe the experimental data. In particular, the first one lies at 150 meV from the main line, while the successive barely visible peak is shifted by 310 meV. The presence of high BE features was recently pointed out also by Kera *et al.*[35] which found, in the case of CuPc thin film, an asymmetric line shape for the a_{1u} hole state; they assign it to the presence of vibrational modes coupled to the photoemission process. In the present gas phase experiment it was possible to distinguish better these extra features. Nonetheless, an exact identification of which molecular vibrations are involved is not a straightforward task. This is because in the energy range where we find the extra excitation (150 meV, ~1210 cm^{-1}) several vibrational modes are possible: according to recent high-resolution electron-energy-loss spectroscopy results[33] our value falls in the energy-loss region characteristic of the in-plane C–C stretching but also very close to energy region of the C–N in-plane stretching.

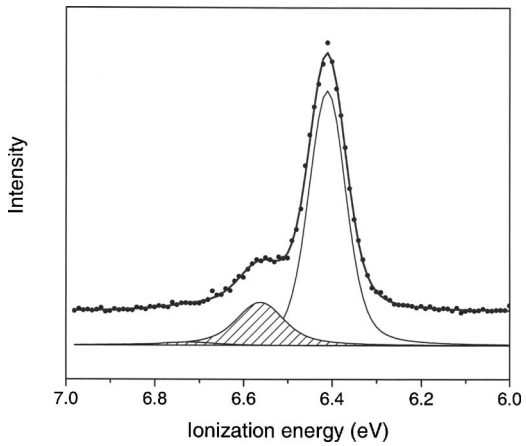

FIG. 5. High resolution photoelectron spectrum of the a_{1u} (HOMO) region collected with a photon energy of 21 eV. The results of the fitting procedure are also reported (solid curves).

Even lacking an exact assignment of the vibrational mode, the observation of excitation of the C–C/N stretching modes and not of the C–H one (~380 meV) can provide important information as well. In particular, it confirms the spatial localization of the a_{1u} on the pyrrole ring predicted by our calculations. In fact, the molecular structure shows that each one of the outer carbon atoms in benzene rings is linked to a hydrogen atom, while only carbon atoms in the pyrrole

TABLE II. Resulting parameters from the fitting procedure presented in Fig. 5

	IE	A	LW	GW
HOMO	6.38	1	0.03	0.08
ν	6.53	0.254	0.09	0.08
ν'	6.69	0.018	0.09	0.08

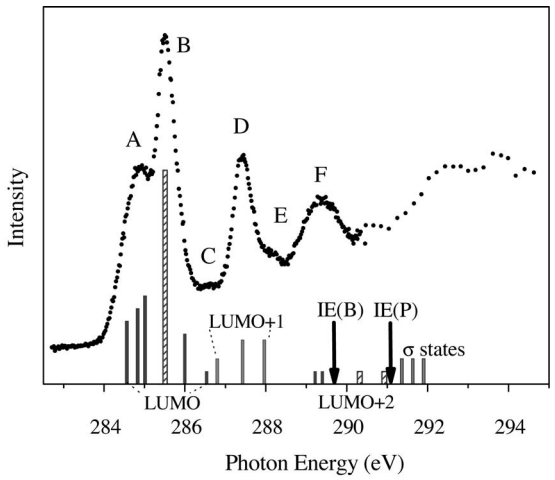

FIG. 6. X-ray absorption spectrum from the C *K* edge collected in total ion yield mode. The main structures detectable are labelled with a letter from A to F. Theoretical bars were arbitrarily superimposed to the experimental data. Different colors account for different final states (LUMO, LUMO+1, etc.), while theoretical energy scale was expanded to compensate the approximations made in the calculations.

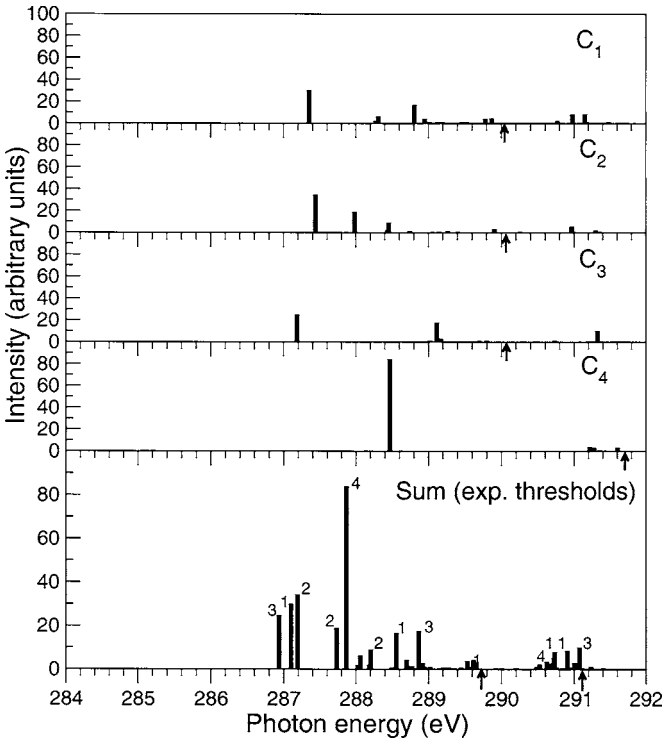

FIG. 7. SCF theoretical calculations on the C *K*-edge absorption spectrum. C1–C4 named panels report on different contributions coming from inequivalent carbon atoms. The arrow indicates the calculated ionization threshold. The lowest panel is the sum of the previous ones with the ionization thresholds aligned to the experimental values (see Fig. 2).

rings can exhibit a C–C and/or C–N in-plane stretching with no involvement of hydrogen atoms. Thus, the hypothesis that the a_{1u} is mainly localized on the C4 carbon atoms is very reasonable and in perfect agreement with the prediction of the DFT calculations, as shown by the spatial distribution reported in Fig. 1, and with previous observations on other metal phthalocyanines, PbPc[13] and NiPc[30].

VI. XANES: EXPERIMENTAL AND THEORETICAL RESULTS

The experimental high-resolution XANES spectrum recorded at the C *K* edge is reported in Fig. 6. An intense two-peak-shaped structure (A and B in the figure) is centered approximately at 285.2 eV, with an A-B energy separation of about 700 meV. At higher photon energies the spectrum shows several features: a weak structure (C) located at about 286.6 eV, a slightly asymmetric structure at 287.4 eV (D) with a shoulder on its high energy side (E), and then a wide feature located approximately at 289.4 eV (F). To the best of our knowledge, this is the first XANES measurement concerning a metal-phthalocyanine in the gas phase. Though XANES was extensively used to determine MPc films molecular orientation it is still debating which orbitals and which contributions from the inequivalent C atoms give rise to the spectral density. In fact, the interpretation of a photoabsorption spectrum is not as straightforward as that of a photoemission spectrum. In XANES the initial ground state as well as the final states have to be taken into account. Thus, the need for a theoretical simulation of the complete photoabsorption spectrum appears evident.

The theoretical spectra obtained by the STEX approach are presented as bar diagrams in Fig. 7. The four upper panels refer to excitations from each group of inequivalent carbon atoms (see the insert in Fig. 2). The larger panel in the lower part of the figure represents the sum of the four different carbon atom contributions, with benzene and pyrrole energy scales calibrated against the experimental ionization energies obtained by XPS (see Fig. 2). Core excitations towards the b_{1g} level (SOMO) are in principle also possible. However, the core orbitals (C 1*s*) and the b_{1g} orbital (mostly Cu $3d_{x^2-y^2}$) exhibit a completely different spatial localization. For this reason the intensity of such excitations at the C *K* edge can be considered very small and they were, as a matter of fact, neglected in our calculations. As the direct result of a STEX calculation are term values rather than excitation energies, a relative shift between benzene and pyrrole XANES spectra can be accepted to partially compensate the missing electron correlation effects. The other approximation (hole overscreening) of the STEX approach gives origin to a "compression" of the computed spectra against the ionization thresholds. To take into account the approximations of the STEX method, in Fig. 6 we superposed the theoretical calculations after applying the following procedure: the energy scales of the benzene (C1, C2, and C3) and pyrrole (C4) calculated XANES spectra were separately expanded keeping fixed the IE values until a good matching with features A and B, respectively, was reached. The good agreement observable in the figure results by multiplying for almost the same factor (about 1.75). The intensities of the bars reported in figure preserve the relative intensity ratios of Fig. 7. Such an experiment-theory comparison allows to assign the main peak B to an intense excitation of π^* character at the C4 site (namely, to the LUMO level), while the first π^* excitations at sites C1–C3 are splitted in intensity and give origin to band A and to the less intense C feature. This splitting stems from the doubly degenerate nature of the unperturbed LUMO level: once the hole is created in the C 1*s*, the

degeneracy is removed and, as a result, two levels (say LUMO and LUMO′) are available. The calculated energy positions for the benzene and the pyrrole C1*s*-LUMO excitations account for the A-B double-shaped peak present in the experimental spectrum. The large D band should be ascribed to excitations towards the LUMO+1 level, mainly concentrated on benzene carbon atoms, in particular, from C1–C3 carbons. The LUMO+1 contribution coming from the pyrrole ring (C4) has a very low intensity and hence was not reported. The weak shoulder E is of difficult assignment, while the wide F structure is probably due to excitations to higher empty molecular orbitals (e.g., LUMO+2) with strong benzene (C1, C2, and C3) character, and also exhibiting pyrrole contribution (C4).

Within the picture exposed, peak A has to be ascribed to core excitations at carbons in the benzene rings and peaks B and C 1*s* excitations at the pyrrole rings. In spite of the stoichiometric ratio between the two inequivalent carbons, the pyrrole-associated peak appears higher in intensity than the benzene-associated one. Large differences regarding the energy separation between the two components are evident as well: the A-B energy difference amounts to 730 meV, that is, approximately half of the chemical shift detected with XPS. Such a behavior can be explained if we carefully look at Fig. 1. In fact, the spatial projection of the LUMOs on the different C atoms is not homogeneous and the dominant C4 contribution is clearly visible. As a consequence, in spite of the B-P stoichiometric ratio of the carbon atoms, transitions from pyrrole C 1*s* orbitals will exhibit a higher intensity. At the same time, when the electron is promoted from a C4 core orbital to the LUMO, a larger screening effect on the 1*s* core hole will occur,[36] thus lowering the chemical shift observed in photoemission from the same core orbitals.

Summarizing, it can be said that the electronic nonequivalence of carbon atoms in CuPc, that characterizes the C 1*s* core level spectrum, also affects the corresponding C *K* edge absorption spectrum. Nevertheless, the localization of the LUMO level in the central part of the molecule modifies the stoichiometric intensity ratio and the energy chemical shift observable in photoemission. On the other hand the LUMO+1 is mainly localized in the outer benzene rings and, as a consequence, a negligible pyrrole LUMO+1 contribution to the absorption spectrum is observed. A support to the interpretation of the D band in terms of excitations towards the LUMO+1 level comes also from considerations about the LUMO-LUMO+1 energy difference. Both theoretically[12] and experimentally[37] such a distance is estimated to be about 2 eV. In our case, if we take as the LUMO position the centroid of the double A-B structure and if we identify the LUMO+1 position with the D structure, a LUMO-LUMO+1 energy distance of 2.2 eV is obtained, thus in good agreement. As far as the LUMO-LUMO+2 distance is concerned, this argument is more difficult to apply, as the wide F structure does not allow a precise energy positioning of the LUMO+2 levels. In literature the distance is given between 3.4 eV[37] and 3.6 eV,[12] which seems slightly lower than our experimentally detectable value.

VII. CONCLUSIONS

The electronic structure of copper phthalocyanine molecule was studied in detail by means of both gas phase experiments (UPS, XPS and XANES) and computational techniques (SCF, DFT and STEX), addressing both occupied and unoccupied orbitals. Contributions from Cu orbitals were singled out and a finer knowledge of the energy level alignment was reached. The coupling of experiment and theory allowed to shed light also on the localization of the outer molecular orbitals. The a_{1u} was seen to be localized on the C atoms of pyrrole rings, while carbon atoms in the benzene rings were shown to be electronically equivalent. As far as the empty states are concerned, STEX calculations provide a satisfactory assignment of the peaks in the XANES spectrum: the doubly degenerate LUMO is shown to split upon the creation of the hole, with its spatial distribution concentrated on the inner ring, thus implying a major intensity for transition from pyrrole carbon atoms (C4), rather than benzene ones (C1, C2, and C3). The LUMO+1 was seen to be localized on benzene rings, while higher energy molecular orbitals exhibit a mixed pyrrole-benzene contribution.

ACKNOWLEDGMENTS

This work was supported partially by the European Research and Training Network "Understanding Nanomaterials from a Quantum Perspective" (NANOQUANT, contract No. MRTN-CT-2003-506842) and partially by MIUR (PRIN 2003028141) and INFM through the "Supporto Elettra" program. We thank A. Morgante and L. Floreano for the technical and scientific assistance for the measurements collected at the ALOISA beamline. We also thank G. Polzonetti for fruitful discussions.

[1] C. D. Dimitrakopoulos, S. Purushothaman, J. Kymissis, A. Callegari, and J. M. Shaw, Science **283**, 822 (1999).
[2] F. Schreiber, J. Phys.: Condens. Matter **16**, R881 (2004).
[3] A. F. Hebard, M. J. Rosseinsky, R. C. Haddon, D. W. Murphy, S. H. Glarum, T. T. M. Palstra, A. P. Ramirez, and A. R. Kortan, Nature (London) **350**, 600 (1991).
[4] M.-S. Liao and S. Scheiner, J. Chem. Phys. **114**, 9780 (2001).
[5] T. Okajima, H. Fujimoto, M. Sumitomo, T. Araki, E. Ito, H. Ishii, Y. Ouchi, and K. Seki, Surf. Rev. Lett. **9**, 441 (2002).
[6] G. Dufour, C. Poncey, F. Rochet, H. Roulet, M. Sacchi, M. De Santis, and M. De Crescenzi, Surf. Sci. **319**, 251 (1994).
[7] A. Cossaro, D. Cvetko, G. Bavdek, L. Floreano, R. Gotter, A. Morgante, F. Evangelista, and A. Ruocco, J. Phys. Chem. B **108**, 14671 (2004).
[8] A. Ruocco, F. Evangelista, M. P. Donzello, and G. Stefani, Phys. Rev. B **67**, 155408 (2003).
[9] H. Peisert, M. Knupfer, and J. Fink, Recent Res. Dev. Appl. Phys. **5**, 129 (2002).
[10] S. Kera, Y. Yabuuchi, H. Yamane, H. Setoyama, K. K. Okudaira, A. Kahn, and N. Ueno, Phys. Rev. B **70**, 085304 (2004).
[11] F. Evangelista, A. Ruocco, V. Corradini, C. Mariani, and M. G. Betti, Surf. Sci. **531**, 123 (2003).
[12] K. A. Nguyen and R. Pachter, J. Chem. Phys. **114**, 10757 (2001).
[13] N. Papageorgiou, Y. Ferro, E. Salamon, A. Allouche, J. M. Layet, L. Giovanelli, and G. Le Lay, Phys. Rev. B **68**, 235105 (2003).
[14] L. Lozzi, S. Santucci, S. De La Rosa, B. Delley, and S. Picozzi, J. Chem. Phys. **121**, 1883 (2004).
[15] Y. Alfredsson, B. Brena, K. Nilson *et al.*, J. Chem. Phys. **122**, 214723 (2005).
[16] J. Ahlund, K. Nilson, J. Schiessling, L. Kjeldgaard, S. Berner, N. Martensson, C. Puglia, B. Brena, M. Nyberg, and Y. Luo, J. Chem. Phys. **125**, 034709 (2006).
[17] H. Agren, V. Carravetta, O. Vahtras, and L. G. M. Patterson, Theor.

Chim. Acta **97**, 14 (1997).
[18] G. Contini, V. Carravetta, V. Di Castro, S. Stranges, R. Richter, and M. Alagia, J. Phys. Chem. A **105**, 7308 (2001).
[19] G. Polzonetti, G. Contini, V. Carravetta, C. Lo Sterzo, A. Ricci, A. Ferri, S. Stranges, and M. De Simone, J. Phys. Chem. A **107**, 6777 (2003).
[20] M. Alagia, C. Baldacchini, M. G. Betti, F. Bussolotti, V. Carravetta, U. Ekstrom, C. Mariani, and S. Stranges, J. Chem. Phys. **122**, 124305 (2005).
[21] A. Mihill, W. Buell, and M. Fink, J. Chem. Phys. **99**, 6416 (1993).
[22] C. Y. Ruan, V. Mastryukov, and M. Fink, J. Chem. Phys. **111**, 3035 (1999).
[23] J. Berkowitz, J. Chem. Phys. **70**, 2819 (1979).
[24] D. Schlettwein, K. Hesse, N. E. Gruhn, P. A. Lee, K. W. Nebesny, N. R. Armstrong, J. Phys. Chem. B **105**, 4791 (2001).
[25] B. L. Westcott, N. E. Gruhn, L. J. Michelsen, D. L. Lichtenberger, J. Am. Chem. Soc. **122**, 8083 (2000).
[26] R. R. Blyth, R. Delaunay, M. Zitnik *et al.*, J. Electron Spectrosc. Relat. Phenom. **101–103**, 959 (1999).
[27] T. X. Carroll, J. Hahne, T. D. Thomas, L. J. Saethre, N. Berrah, J. Bozek, and E. Kukk, Phys. Rev. A **61**, 042503 (2000).
[28] T. K. Sham, B. X. Yang, J. Kirz, and J. S. Tse, Phys. Rev. A **40**, 652 (1989).
[29] M. W. Schmidt, K. K. Baldridge, J. A. Boatz *et al.*, J. Comput. Chem. **14**, 1347 (1993).
[30] F. W. Kutzler and D. E. Ellis, J. Chem. Phys. **84**, 1033 (1986).
[31] DALTON, a molecular electronic structure program, Release 2.0 (2005), see http://www.kjemi.uio.no/software/dalton/dalton.html
[32] S. Carniato, Ph.D. thesis Université Paris VI, 1992.
[33] J. J. Yeh and I. Lindau, At. Data Nucl. Data Tables **32**, 1 (1985).
[34] T. S. Ellis, K. T. Park, S. L. Hubert, M. D. Ulrich, and J. E. Rowe, J. Appl. Phys. **95**, 982 (2004).
[35] S. Kera, H. Yamane, I. Sakuragi, K. K. Okudaira, and N. Ueno, Chem. Phys. Lett. **364**, 93 (2002).
[36] H. Oji, R. Mitsumoto, E. Ito, H. Ishii, Y. Ouchi, K. Seki, T. Yokoyama, T. Ohta, and N. Kosugi, J. Chem. Phys. **109**, 10409 (1998).
[37] I. G. Hill, A. Kahn, Z. G. Soos, and A. Pascal, Jr., Chem. Phys. Lett. **327**, 181 (2000).